Journal of *Marine Science and Engineering*

MDPI

Article

Bio-Based Adhesives for Wooden Boatbuilding

Pasqualino Corigliano [1,*], Vincenzo Crupi [1], Serena Bertagna [2] and Alberto Marinò [2]

[1] Department of Engineering, University of Messina, 98166 Messina, Italy; crupi.vincenzo@unime.it
[2] Department of Engineering and Architecture, University of Trieste, 34127 Trieste, Italy; sbertagna@units.it (S.B.); marino@units.it (A.M.)
* Correspondence: pcorigliano@unime.it

Abstract: The aim of the present investigation was to assess the behaviour of strip-planked parts by comparing wooden specimens glued using two different bio-based adhesives with wooden specimens glued using a conventional epoxy resin generally used in boatbuilding. Experimental tests in accordance with UNI EN standards were performed in order to evaluate mechanical properties such as tensile strength, shear strength, elastic modulus and shear modulus. In addition, compression shear tests were performed in order to assess the shear modulus of the adhesives. The obtained results demonstrate that the mechanical properties of the investigated bio-based adhesives are comparable to, and sometimes better than, the conventional epoxy resin. Moreover, the experimental results give useful information for the design of wooden boats when the strip-planking process is used. Furthermore, a new procedure to assess the shear modulus of elasticity and shear strength, using the application of compression loadings, was proposed. The results were compared to standard lap-joint tests and showed even lower dispersion. Consequently, the testing procedure proposed by the authors is valid to assess shear properties under compression loading, and it can be applied in most laboratories since it involves the use of common testing devices.

Keywords: boatbuilding; laminated wood; composite materials; strip-planking; bio-based adhesives; green materials

Citation: Corigliano, P.; Crupi, V.; Bertagna, S.; Marinò, A. Bio-Based Adhesives for Wooden Boatbuilding. *J. Mar. Sci. Eng.* **2021**, *9*, 28. https://doi.org/10.3390/jmse9010028

Received: 22 November 2020
Accepted: 26 December 2020
Published: 30 December 2020

1. Introduction

Fibre-reinforced polymers (FRPs) are the most used materials for the construction of small-size vessels. Fibreglass plays a leading role within this scope, since its performance, together with production characteristics and low cost, have made it an undisputed material for boat production [1]. Furthermore, the choice of the right adhesive is of utmost importance for many marine sectors [2–5] because the adhesive joints are generally the weakest spots in the structures [6].

FRP boats currently make up 90% of the circulating boats, despite the issue of their end-of-life management. As reported in [7], they represent a significant problem for the environment and related health issues. Unfortunately, it is common to dispose of FRP vessels in landfill or by sinking, although such procedures have a significant impact on the ecosystem. Some recycling and reuse technologies have been studied and developed [8–11], even though the heterogeneous nature of matrices and reinforcements complicates such processes [12]. As a consequence, these recycling techniques involve high costs, questionable environmental impact, and lower quality of the attained products [13]. In addition, FRP materials use a significantly high amount of energy for their production [14]. All these aspects must be taken into account while approaching the life cycle assessment (LCA) of a vessel; raw material production and end-of-life alternatives (reuse, recycling, and disposal) are fundamental to define the complete life cycle of vessels [15].

Thus, in order to follow the increasingly important trend of minimising environmental impact and promoting sustainable development in the boatbuilding industry [16], the introduction of both eco-friendly materials and construction technologies is necessary.

Within this context, wood, which can be considered the most ancient material used for boatbuilding, presents the following advantages: it requires low amounts of energy for growth and production as compared to FRP and steel and it is a renewable resource and has a net carbon negative footprint [14]. It is currently reacquiring its appeal, and several studies focused on wooden boats have been recently proposed [6,17,18].

Knowledge of the quality and mechanical properties of wooden laminates is of extreme significance [19], and several studies reporting various wood essences are present in the literature. In particular, the mechanical properties of Iroko wood [20] and Iroko laminates [21] used in boatbuilding have been investigated, while evaluations of the mechanical properties of Douglas fir and Japanese cedar lumber are reported in [22,23]. The impact responses of wood-based sandwich structures are investigated in [24,25].

Among all the wood construction processes available, the strip-planking technique is particularly advantageous, due to the possibility of exploiting the material properties by orienting the wood's natural grains in the most advantageous direction. Furthermore, it involves an easy technological process to build a strong and rigid wooden structure with a remarkable strength-to-weight ratio, high fatigue resistance and resilience [7,26].

The strip-planking technique consists of stratifying a number of wood strips and veneers with different thickness, with the natural grains properly oriented. The wood strips and veneers are kept together by means of a proper adhesive. The first step involves arranging a pattern made of a series of transversal frames in order to reproduce the boat hull form and to lay the definitive stringers (Figure 1a). The transversal frames serve as support for the longitudinal strips, which run in the fore-aft direction (Figure 1b,c). The external surface of the strip layer, after being smoothed by grinding, represents the base for the successive veneer layers (Figure 1d), which consist of wide, thin, highly flexible bands that easily fit the hull shapes. However, it is known that sea water exposure is a very important aspect that can affect material and adhesive strengths. Thus, a gel-coated layer and antifouling paint are applied to the external surface of the hull, so the direct contact between sea water and wood is avoided, as shown in Figure 2a–d.

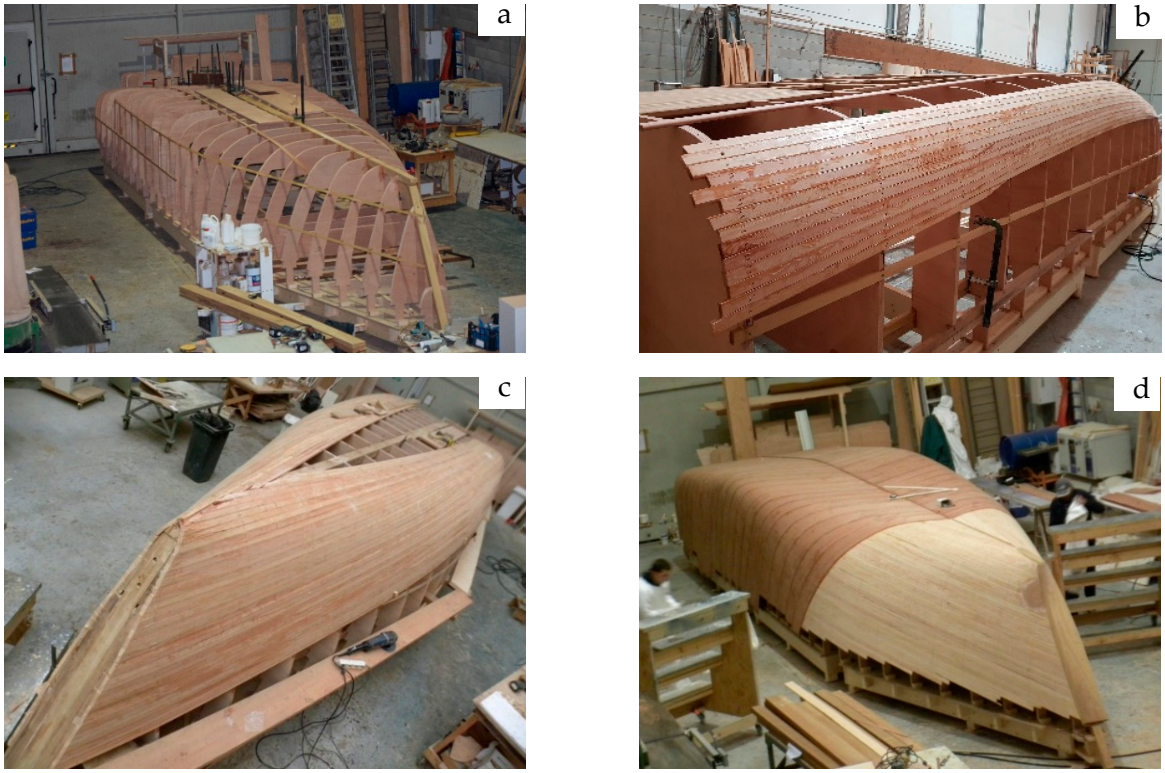

Figure 1. Phases of the construction of a strip-planked hull.

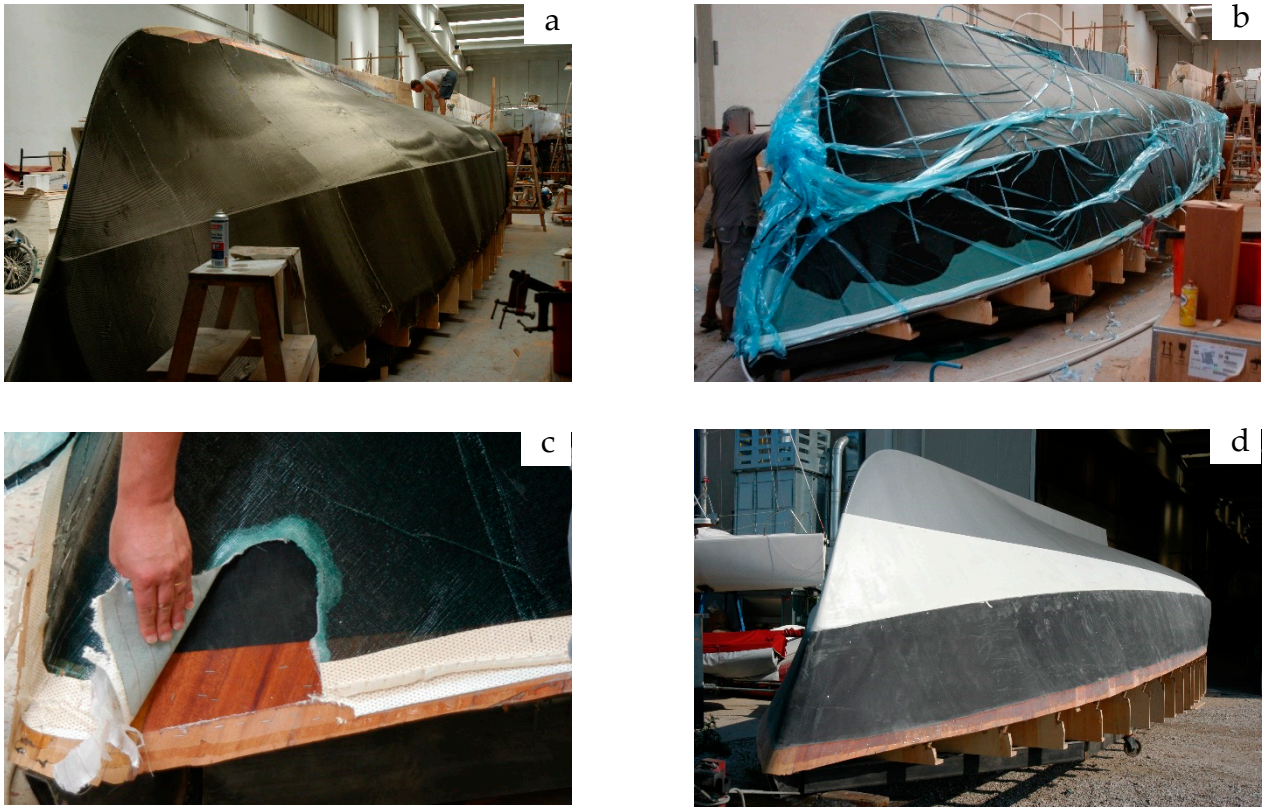

Figure 2. External gel-coating of the hull.

Commonly, longitudinal strips have a rectangular cross section having edges arranged with semi-circular mouldings (one concave and the other convex), in order to both fit the hull transversal curvature and guarantee a better bonding between adjacent strips. Ideally, strips should have a length that allows them to run from stern to bow in a unique piece, but this situation hardly occurs; often, strips must be jointed together. Generally, scarf joints are used, with the strip ends bevelled (slope approximately 1:7), overlapped and glued together.

Strip-planking technology is particularly advantageous for one-off projects; it requires more modest skills with respect to traditional wooden construction processes.

Despite the fact that wood is a "green" material, wooden construction generally involves the use of conventional resins as adhesives. In particular, the use of epoxy resins lowers the eco-friendly feature of the final products. Because of this, it is necessary to look for other adhesives that are less environmentally detrimental. Bio-based epoxy resins represent one of the most interesting solutions. Since the use of these polymers is relatively innovative in the nautical field, their mechanical properties have to be assessed through proper tests. Such properties will be used to perform structural sizing, in accordance with the requirements provided by classification societies and international standards. In particular, Germanischer Lloyd gives criteria based on a comparison of the stress of each individual layer and the average breaking stress (tension/compression) of the material [27].

Therefore, focused research was carried out to assess the mechanical properties of two different bio-based adhesives through experimental tests, and compare them with the properties of a conventional epoxy resin. Two of the most frequently adopted wood essences in strip-planked boats were chosen (i.e., Douglas fir and Mahogany Sapele). Among the mechanical properties, particular attention was given to the shear elastic modulus and the shear strength. To this end, standard tests on lap-jointed specimens were performed, while an ad hoc test was proposed for the determination of the shear modulus

and the shear strength of the adhesive by means of a system based on a compressive loading test-setup, which is easily replicated with common laboratory facilities.

2. Materials and Methods

2.1. Materials

The essences chosen were among the most common types of wood used in strip-planking construction technology. Hence, the different wood essences investigated were Douglas fir and Mahogany Sapele. The first is an evergreen conifer species belonging to softwoods and is commonly used for strips, while the latter is a hardwood commonly used for veneers. Their main properties are reported in Table 1. Therefore, a typical configuration of a strip-planked boat consists of Douglas fir longitudinal strips combined with Mahogany veneers oriented at $\pm 45^{\circ}$.

Table 1. Properties of the employed woods.

Property	Douglas Fir	Mahogany Sapele
Origin	North West of America	Ivory Coast, Congo, Nigeria, Ghana
Grain	Straight	Slightly interlocked
Log diameter [cm]	From 50 to 80	From 70 to 120
Specific gravity *	0.54 ± 0.04	0.69 ± 0.04
Fibre saturation point [%]	27	29
Crushing strength [MPa]	50 ± 6	62 ± 7
Static bending strength * [MPa]	91 ± 6	102 ± 11
Modulus of elasticity * [MPa]	$16{,}800 \pm 1550$	$13{,}960 \pm 2403$
Treatability (according to Standard EN 350:2016 [28])	Class 4: not permeable	Class 3: poorly permeable

* at 12% moisture content.

The conventional adhesive employed was the following bi-component system:

- Epoxy resin:
  - Bisphenol A Diglycidyl ether;
  - Epoxide derivatives mw < 700.
- Curing agent:
  - Alkyl ether polyamine;
  - M-Xylene diamine;
  - Isophorone diamine.

The bio-based epoxy adhesives chosen for testing had characteristics, in terms of mechanical properties, as close as possible to the chosen conventional epoxy resin, which is commonly used as an adhesive in strip-planking technology.

Two bio-based epoxy adhesives, produced by Cardolite Corporation (Antwerp, Belgium) and having resin matrix and amine hardener made from high amounts of renewable resources (cashew nutshell), were selected. The main resin component (Cardanol) is obtained from cashew nut shell liquid (CNSL), a phenolic material that does not interfere with the food chain. Cardanol is characterised by a long aliphatic side chain that provides excellent water, salt-water, and moisture resistance, good flexibility, low viscosity, extended pot life, and excellent corrosion protection. The bio-based epoxy adhesives chosen are the FormuLITE 2501LCA + UltraLITE 2009HSF (referred as "A" in this paper), and the FormuLITE 2501A + FormuLITE 2002B (herein referred to as "B"). They have a natural-origin content equal to 34.8% and 45.4%, respectively. In particular, adhesive A was specifically modified, in terms of content of accelerant substances, for the purposes of the present research by the company AEP Polymers, which is scientific advisor to and industrial partner of the Cardolite Corporation.

The properties of the compared adhesives are reported in Table 2.

Table 2. Properties of the investigated adhesives.

	Conventional Epoxy Adhesive	Bio-Based Adhesives	
	C	**A**	**B**
Pot life [min]	-	-	-
at 20 °C	37	-	-
at 25 °C	-	18	58
Viscosity (of the mixes) [mPa s]	-	-	-
at 20 °C	800	-	-
at 25 °C	-	1300	1100
at 40 °C	240	600	377
Ultimate T_g [°C]	62	75	73
Tensile strength [MPa]	64	64	52
Tensile modulus [MPa]	2850	2886	2599
Tensile elongation at F_{max}/at break [%]	3.6/6.9	4.51/6.27	4.3/11.3
Flexural strength [MPa]	102	(117) *	73
Flexural modulus [MPa]	3070	(2921) *	2104
Natural-origin content [% wt]	-	34.8	45.4

* The values refer to a similar adhesive produced by the Cardolite Corporation.

It is possible to see that the bio-adhesives have higher values of viscosity with respect to the conventional epoxy adhesive. This implies the presence of longer molecular chains in the structure of the bio-based polymers. However, the viscosity difference for the three investigated adhesives does not have a significant impact during their application in situ according to the working experience of wooden boatbuilders.

2.2. Methods

In order to identify the experimental tests to perform, three different Standards for mechanical tests on wood adhesives were selected:

- UNI EN 408: "Structural timber and glued laminated timber–Determination of some physical and mechanical properties" [29], used for tensile tests on scarf-jointed strips;
- UNI EN 302-1: "Adhesives for load-bearing timber structures Part 1–Determination of longitudinal tensile shear strength" [30], used for tensile-shear tests on lap-jointed strips;
- ASTM D905-03: "Standard Test Method for Strength Properties of Adhesive Bonds in Shear by Compression Loading" [31], used to set up the ad hoc compressive loading tests.

All the experimental tests were performed using a servo-hydraulic Instron testing device with a load-cell of 250 kN and a resolution of 1% on the recorded load value.

The aim of the tensile tests on scarf-jointed strips was to assess the characteristic value of both the tensile strength and the tensile elastic modulus. The specimen geometry used for this kind of test is represented in Figure 3a; tabs were placed at the two ends of the specimen in order to avoid crushing caused by the grips. The test was performed at a displacement rate of 2.5 mm/min.

For the tensile-shear tests, the specimens were made of two rectangular-shaped strips, glued together by means of a lap joint (Figure 3b). The specimens were placed symmetrically between the grips of the testing machine positioned at a distance in the range of 50 to 90 mm. The experimental tests were performed at a constant crosshead speed not exceeding 5 mm/min, such that the time required to reach failure was in the range of 30 to 90 s.

The shear tests by compression loading (i.e., compression-shear tests) were performed based on ASTM D905-03. This Standard was used as a guide to identify an ad hoc specimen that could be tested with common laboratory machinery. Specifically, the specimens were made of three square-shaped panels, glued together in order to form a parallelepiped as shown in Figure 3c. During the test, a compression load was applied both on the upper

surface of the central panel and on the lower surfaces of the two lateral panels, using three equal steel bars. The crosshead motion was set at a rate of 5 mm/min until failure.

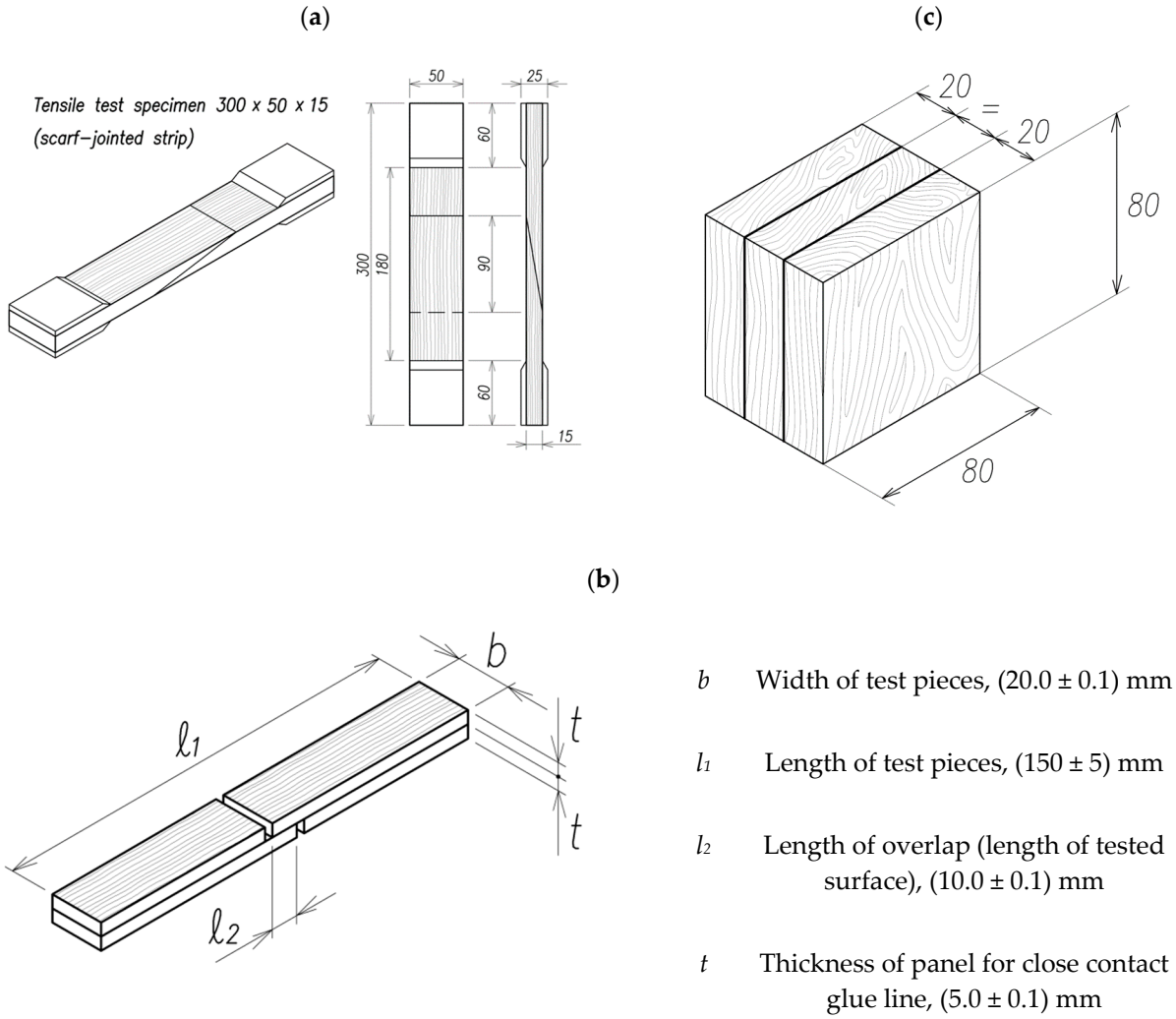

Figure 3. Geometry and dimensions of the tested specimens (units in mm). (**a**) Scarf-joint specimen. (**b**) Tensile-shear test specimen. (**c**) Compression-shear test specimen.

In order to have clear and easily readable results, all the specimens were indexed with a code containing information about the wood essence, the adhesive used and the test type. Each specimen had an alphabetic code (letter meanings given in Table 3) followed by a number that identifies the specific specimen.

Table 3. Letter meanings of the specimen code.

Test Code	Wood Code	Adhesive Code
CS Compression Shear	**F** Douglas Fir	**A** Bio-based epoxy resin A
TS Tensile Shear	**M** Mahogany Sapele	**B** Bio-based epoxy resin B
TJ Tensile Scarf-Joint	-	**C** Conventional epoxy resin

The test pieces were manufactured using the two essences (F,M) and the three adhesives (A,B,C).

In order to properly prepare wood panels for the manufacture of the specimens, surfaces were sanded with sandpaper having a grit size equal to 60 in order to perform a primary sanding of the rough wood. Then, the adhesive was applied as a uniform layer.

Mean values ($\bar{x}$) and root mean square (RMS) values were calculated for each evaluated mechanical property, and their probability density function is reported in Appendix A as a normal distribution. However, to consider the dispersion of the experimental results, threshold characteristic values needed to be calculated.

The characteristic value of a population was assumed, within this context, to be the value corresponding to the 5-percentile (i.e., the value with 5% probability of occurrence).

The 5-percentile value for data normally distributed is determined as follows:

$$x_k = \bar{x} - 1.645\ \mathrm{RMS} \quad (1)$$

3. Results and Discussion

3.1. Tensile Properties of Scarf-Jointed Strips

Nine specimens for each wood essence–adhesive system (F/M–A/B/C) were tested. Figure 4 shows a specimen at the end of the test.

Figure 4. Scarf-joint after rupture.

For each specimen, the test results were represented by a force-displacement graph (Figure 5).

The tensile strength, $\sigma_{t,0}$, was calculated in accordance with UNI EN 408 [29] as follows:

$$\sigma_{t,0} = F_{max}/A_0 \quad (2)$$

where F_{max}. is the maximum load reached during the test and A_0 is the area of the cross section of the specimen. Furthermore, the modulus of elasticity in tension, $E_{t,0}$, was calculated as follows:

$$E_{t,0} = \frac{l_1(F_2 - F_1)}{A_0(w_2 - w_1)} \quad (3)$$

where l_1 is the reference length; $(F_2 - F_1)$ is the load increase on the straight part of the force-displacement curve; A_0 is the area of the cross section of the specimen; $(w_2 - w_1)$ is the displacement increase corresponding to the range $(F_2 - F_1)$. The load increase was chosen

for each test in order to obtain a coefficient of determination, R^2, of the load-displacement linear regression higher than 0.99.

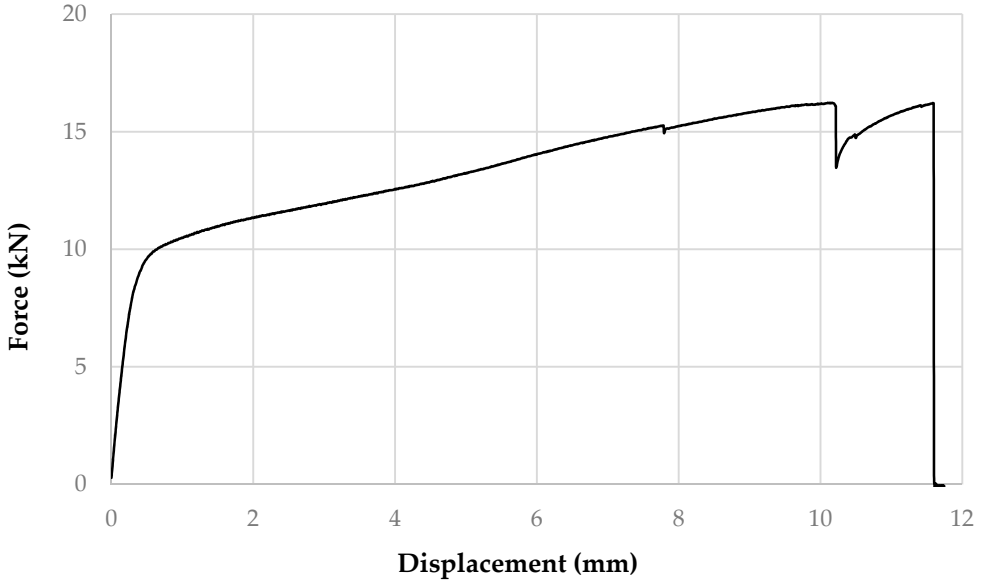

Figure 5. Typical force-displacement graph of a scarf-joint test (TJFA5).

The results obtained for each wood essence–adhesive system are reported in Tables 4 and 5.

Table 4. Results for Douglas fir scarf-joint tensile properties.

		$E_{t,0}$ [MPa]	$\sigma_{t,0}$ [MPa]
(TJFA): Douglas fir–bio-adhesive A	$\bar{x}$	6556	24.68
	RMS	419	7.072
	x_k	5866	13.04
(TJFB): Douglas fir–bio-adhesive B	$\bar{x}$	6279	18.25
	RMS	490	1.306
	x_k	5473	16.10
(TJFC): Douglas fir–conventional adhesive C	$\bar{x}$	6392	21.74
	RMS	572	1.877
	x_k	5451	18.65

Table 5. Results for Mahogany Sapele scarf-joint tensile properties.

		$E_{t,0}$ [MPa]	$\sigma_{t,0}$ [MPa]
(TJMA): Mahogany Sapele–bio-adhive A	$\bar{x}$	8926	50.90
	RMS	506	7.196
	x_k	8093	39.07
(TJMB): Mahogany Sapele–bio-adhesive B	$\bar{x}$	8853	48.31
	RMS	281	6.375
	x_k	8391	37.82
(TJMC): Mahogany Sapele–conventional adhesive C	$\bar{x}$	8071	49.99
	RMS	317	9.437
	x_k	7550	34.46

For the Douglas fir essence, the values of the modulus of elasticity in tension $E_{t,0}$ for the three adhesives are nearly equal; the bio-adhesive A provides the highest value.

However, the value of the tensile strength, $\sigma_{t,0}$, for the bio-adhesive A, even though it is the highest, is affected by a higher dispersion that results in the value of the 5-percentile tensile strength being the lowest. The performances of the bio-adhesive B and the conventional adhesive C are more similar: the tensile strength of the bio-adhesive B is slightly inferior to the value of the conventional one, while the values for the modulus of elasticity are nearly equal.

For the Mahogany Sapele, while the proposed bio-based adhesives and the conventional epoxy presented comparable performances, the two bio-based adhesives seemed to perform better, having higher elasticity moduli and tensile strength than the conventional epoxy adhesive.

It is important to note that, in almost all cases for the two essences, the specimen failure did not occur in correspondence with the scarf joint. Therefore, the three adhesives tested presented a very good response to the tensile load.

3.2. Shear Properties of Lap Joints by Tensile Loading

Seven specimens for each wood essence–adhesive system (F/M–A/B/C) were tested. Figure 6 shows a specimen during the test.

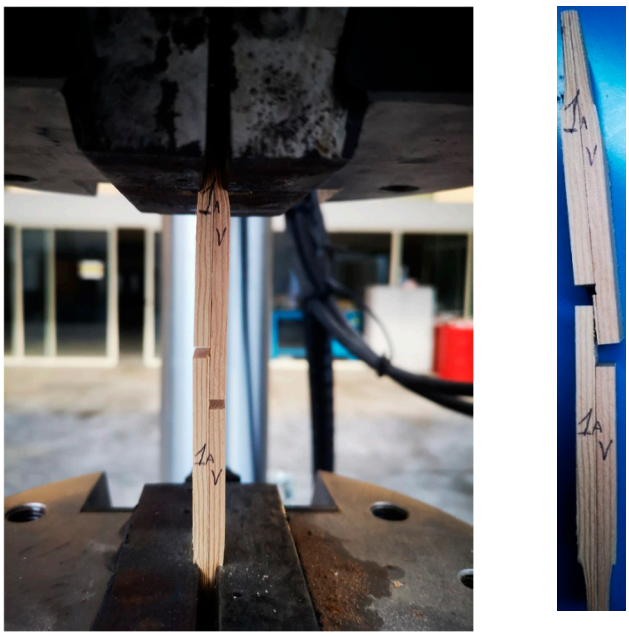

(**a**) during the test (**b**) after rupture

Figure 6. Lap joint test. (**a**) during the test, (**b**) after rupture.

For each specimen, the test results were represented by a force-displacement graph (Figure 7).

For each specimen, the mean shear stress, $\bar{\tau}$ was calculated in accordance with UNI EN 302-1 [30] as $\bar{\tau} = F_{max}/A$, where F_{max} is the applied load at failure and A is the bonded surface area.

Furthermore, the shear modulus, G, for the adhesive layer was calculated as follows:

$$G = \frac{\bar{\tau}}{\gamma} = \frac{\Delta F/A}{\Delta w/c} = \frac{c(F_2 - F_1)}{A(w_2 - w_1)} \quad (4)$$

where $\bar{\tau}$ is the mean shear stress and γ is the shear strain; c is the mean adhesive layer thickness (measured from the specimen sample and equal to 0.199 mm); $(F_2 - F_1)$ is the load increase on the straight part of the force-displacement curve; A is the bonded surface area; $(w_2 - w_1)$ is the displacement increase corresponding to the range $(F_2 - F_1)$.

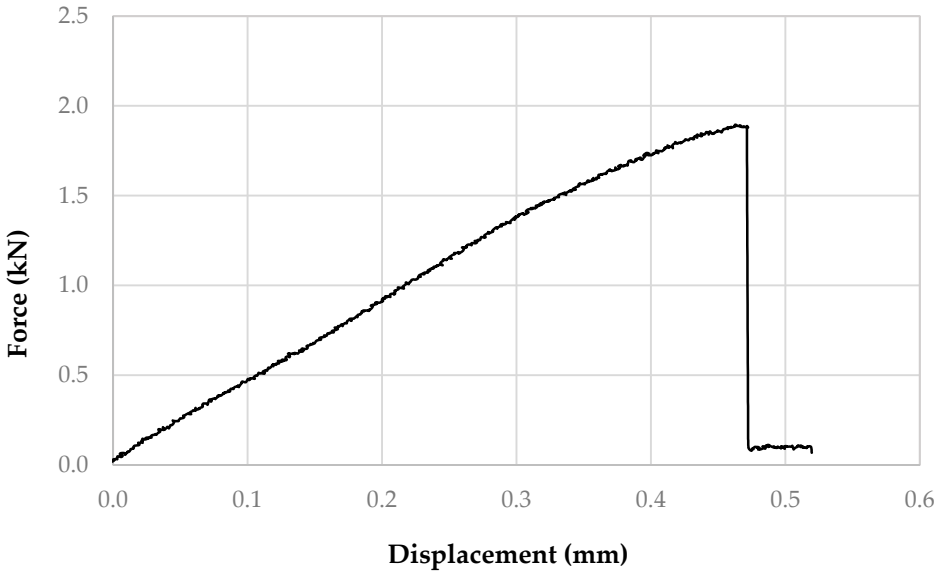

Figure 7. Typical force-displacement graph of a lap joint test (TSMA01).

The authors introduced Equation (4), since UNI EN 302-1 does not provide a formula to evaluate the shear modulus, G, in tensile test.

The load increase was chosen for each test in order to obtain a coefficient of determination, R^2, of the load-displacement linear regression higher than 0.99.

The obtained results are reported in Tables 6 and 7.

Table 6. Results for Douglas fir lap joint shear properties by tensile loading.

		G [MPa]	$\bar{\tau}$ [MPa]
(TSFA): Douglas fir–bio-adhesive A	$\bar{x}$	4.930	4.854
	RMS	0.853	0.674
	x_k	3.526	3.744
(TSFB): Douglas fir–bio-adhesive B	$\bar{x}$	3.760	8.465
	RMS	0.493	1.394
	x_k	2.949	6.171
(TSFC): Douglas fir–conventional adhesive C	$\bar{x}$	4.531	7.916
	RMS	0.987	0.795
	x_k	2.907	6.609

Table 7. Results for Mahogany Sapele lap joint shear properties by tensile loading.

		G [MPa]	$\bar{\tau}$ [MPa]
(TSMA): Mahogany Sapele–bio-adhesive A	$\bar{x}$	3.598	8.180
	RMS	0.701	2.254
	x_k	2.446	4.472
(TSMB): Mahogany Sapele–bio-adhesive B	$\bar{x}$	4.734	8.309
	RMS	0.473	2.702
	x_k	3.957	3.865
(TSMC): Mahogany Sapele–conventional adhesive C	$\bar{x}$	4.143	9.078
	RMS	1.111	3.506
	x_k	2.314	3.311

For the Douglas fir, the bio-adhesive B and the conventional adhesive provided comparable performances. The values for the shear stress were similar (for the bio-adhesive B, the value was slightly inferior to the value for the conventional one), whereas the values of the shear modulus were nearly equal. The situation was different for the bio-adhesive A, which provided a higher value of the shear modulus but a value of the shear strength that was almost half of the others.

For the Mahogany Sapele, the bio-adhesive A provided the best result in terms of shear stress, but the bio-adhesive B provided the best result in terms of shear modulus. The conventional adhesive provided the worst results for both tests. Based on the results, the bio-adhesive B seemed to be the best compromise.

3.3. Shear Properties of Adhesives by Compression Loading

As mentioned, ASTM D905-03 [31] was used as a guide to identify an ad hoc specimen that could be tested with common laboratory machinery. Thus, compression-shear tests were performed on a specimen made of three panels, as shown in Figure 8. Nine specimens for each wood essence–adhesive system (F/M–A/B/C) were tested.

Figure 8. Compression-shear test.

For each specimen, the test results were represented by a force-displacement graph (Figure 9).

For each specimen, the mean shear stress, $\bar{\tau}$, was calculated as $\bar{\tau} = F_{max}/A$, where F_{max} is the applied load at failure and A is the bonded surface area. The shear modulus, G, in compression test was calculated by means of Equation (4), considering the mean adhesive layer thickness, c, equal to 0.388 mm (as evaluated from specimen sample). The results are reported in Tables 8 and 9.

For the Douglas fir, the bio-adhesive B and the conventional one provided comparable performances; the values for the shear stress and for the shear modulus were quite similar. The situation was different for the bio-adhesive A, which provided a higher value of the shear stress, but a value of the shear modulus that was considerably inferior to the others.

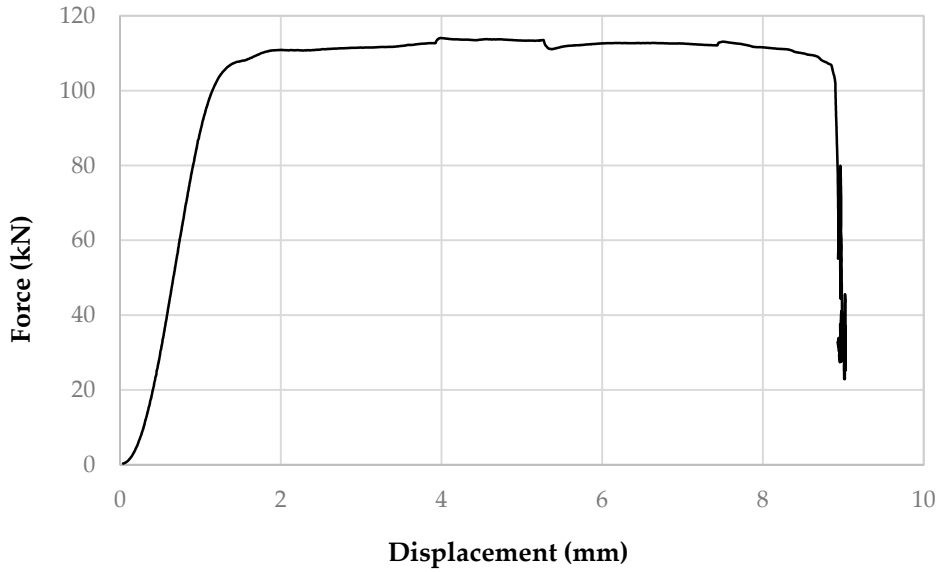

Figure 9. Typical force-displacement curve of a compression-shear test (CSMB07).

Table 8. Results for Douglas fir shear properties by compression-shear tests.

		G [MPa]	$\bar{\tau}$ [MPa]
(CSFA): Douglas fir–bio-adhesive A	$\bar{x}$	3.442	7.875
	RMS	0.442	0.081
	x_k	2.715	7.741
(CSFB): Douglas fir–bio-adhesive B	$\bar{x}$	3.522	6.536
	RMS	0.192	0.395
	x_k	3.206	5.887
(CSFC): Douglas fir–conventional adhesive C	$\bar{x}$	3.880	7.409
	RMS	0.285	0.306
	x_k	3.411	5.352

Table 9. Results for Mahogany Sapele shear properties by compression-shear tests.

		G [MPa]	$\bar{\tau}$ [MPa]
(CSMA): Mahogany Sapele–bio-adhesive A	$\bar{x}$	3.196	9.308
	RMS	0.254	0.321
	x_k	2.778	8.780
(CSMB): Mahogany Sapele–bio-adhesive B	$\bar{x}$	3.431	8.724
	RMS	0.447	0.237
	x_k	2.695	8.334
(CSMC): Mahogany Sapele–conventional adhesive C	$\bar{x}$	3.618	8.373
	RMS	0.271	0.686
	x_k	3.172	7.245

For the Mahogany Sapele, the bio-adhesives A and B provided similar results; they were best in terms of shear stress but worst in terms of shear modulus. The conventional adhesive gave the best performance in terms of shear modulus and the worst in terms of shear stress.

4. Conclusions

Bio-based adhesives represent an important way to enhance the eco-friendly capability of wooden boats, and the strip-planking technique represents one of the most advantageous technologies for their use. With reference to this technology, two wood essences typically used were coupled with two types of bio-based adhesives. The mechanical properties were compared to the mechanical properties of the same wood essences glued by means of a conventional epoxy resin. The results were satisfactory and in almost all cases the obtained properties were comparable.

The following conclusions can be drawn.

For the tensile tests on scarf-jointed strips:

- The obtained values of the modulus of elasticity in tension were nearly equal for all the investigated joints.
- The bio-adhesive B was the best alternative to the conventional adhesive for both Douglas fir and Mahogany Sapele.

For the tensile-shear tests:

- The three adhesives gave similar results with no significant differences.
- The bio-adhesive B was the best alternative to the conventional adhesive for both Douglas fir and Mahogany Sapele.

For the shear tests by compression loading:

- The bio-adhesive A was the best in terms of shear stress and the worst in terms of shear modulus for Douglas fir, while the bio-adhesive B was the best compromise as it gave a higher shear stress and a slightly lower shear modulus with respect to the conventional adhesive.
- The bio-adhesive A was the best compromise for Mahogany Sapele as it presented the highest shear stress and a slightly lower shear modulus with respect to the conventional adhesive.

Another important aspect that is worth noting regards the procedures used to perform the compression-shear tests and to evaluate the shear modulus, G, both introduced by the authors. The results in terms of mean value of shear stress, $\overline{\tau}$, and shear modulus, G (evaluated through Equation (4)), obtained through tensile-shear and compression-shear tests were very similar. Furthermore, the tensile-shear test gave results that have higher dispersions; consequently, the values seemed to be less precise than the ones obtained through the shear test by compression loading. Therefore, it is possible to assume that the testing procedure proposed by the authors and described in Section 3.3 is valid to assess shear properties under compression loading and could be applied in most laboratories, since it involves the use of common testing devices.

Ultimately, it can be concluded that bio-based adhesives represent a valid alternative, being a more ecological solution that offers comparable mechanical properties to conventional adhesives when they are applied together with laminated Douglas fir and Mahogany wood for the strip-planking used in boatbuilding.

Author Contributions: Conceptualization, S.B. and A.M.; methodology, S.B. and A.M.; validation, P.C., V.C., S.B. and A.M.; formal analysis, S.B.; investigation, P.C. and V.C.; resources, P.C., V.C., S.B. and A.M.; data curation, P.C.; writing—original draft preparation, P.C.; writing—review and editing, P.C., V.C., S.B. and A.M.; visualization, S.B.; supervision, V.C. and A.M.; project administration, A.M.; funding acquisition, S.B. and A.M. All authors have read and agreed to the published version of the manuscript.

Funding: This research was funded by CEI–CENTRAL EUROPEAN INITIATIVE Executive Secretariat, through the B_B Trans. Blue Innovation Voucher Scheme, within the project "Interreg ADRION BLUE_BOOST", Priority Axis: Innovative and smart region.

Institutional Review Board Statement: Not applicable.

Informed Consent Statement: Not applicable.

Data Availability Statement: Data is contained within the article.

Acknowledgments: This research was supported by the shipyard Alto Adriatico Custom srl in Monfalcone (Italy) and the company AEP Polymers srl in Area Science Park, Basovizza-Trieste (Italy).

Conflicts of Interest: The authors declare no conflict of interest. The funders had no role in the design of the study; in the collection, analyses, or interpretation of data; in the writing of the manuscript, or in the decision to publish the results.

Nomenclature

T_g	Glass transition temperature [°C]
$\overline{x}$	Mean value
RMS	Root mean square
x_k	Characteristic value (5-percentile)
$\sigma_{t,0}$	Tensile strength parallel to grain [MPa]
F_{max}	Maximum load reached during the test [N]
A_0	Area of the cross section of the specimen [mm^2]
$E_{t,0}$	Modulus of elasticity in tension parallel to grain [MPa]
l_1	Reference length [mm]
$(F_2 - F_1)$	Load increase on the straight part of the force-displacement curve [MPa]
$(w_2 - w_1)$	Displacement increase corresponding to the range $(F_2 - F_1)$ [mm]
R^2	Coefficient of determination
$\overline{\tau}$	Mean shear stress [MPa]
G	Shear modulus [MPa]
A	Bonded surface area [mm^2]
γ	Shear strain
c	Mean adhesive layer thickness [mm]

Appendix A

A linear regression analysis was performed based on the force-displacement data, considering only the data of the initial region (in the range of $0.10 \div 0.40\ F_{max}$). Within this, a sub-region was chosen in such a way as to get a regression straight-line with a coefficient of determination, R^2, greater than 0.99.

The various experimental quantities constitute a series of x-data, which can be statistically analysed by considering a normal (or Gaussian) distribution.

For a x-data population normally distributed, the probability density function, pdf(x), is expressed as follows:

$$\mathrm{pdf}(x) = \frac{1}{RMS\sqrt{2\pi}} \exp\left(\frac{(x - \overline{x})}{2MS}\right)^2 \quad \text{(A1)}$$

where $\overline{x}$ is the mean value of the x-data population, MS is the mean square and RMS is the root mean square (or standard deviation).

The statistical analysis performed is reported in Figures A1–A6.

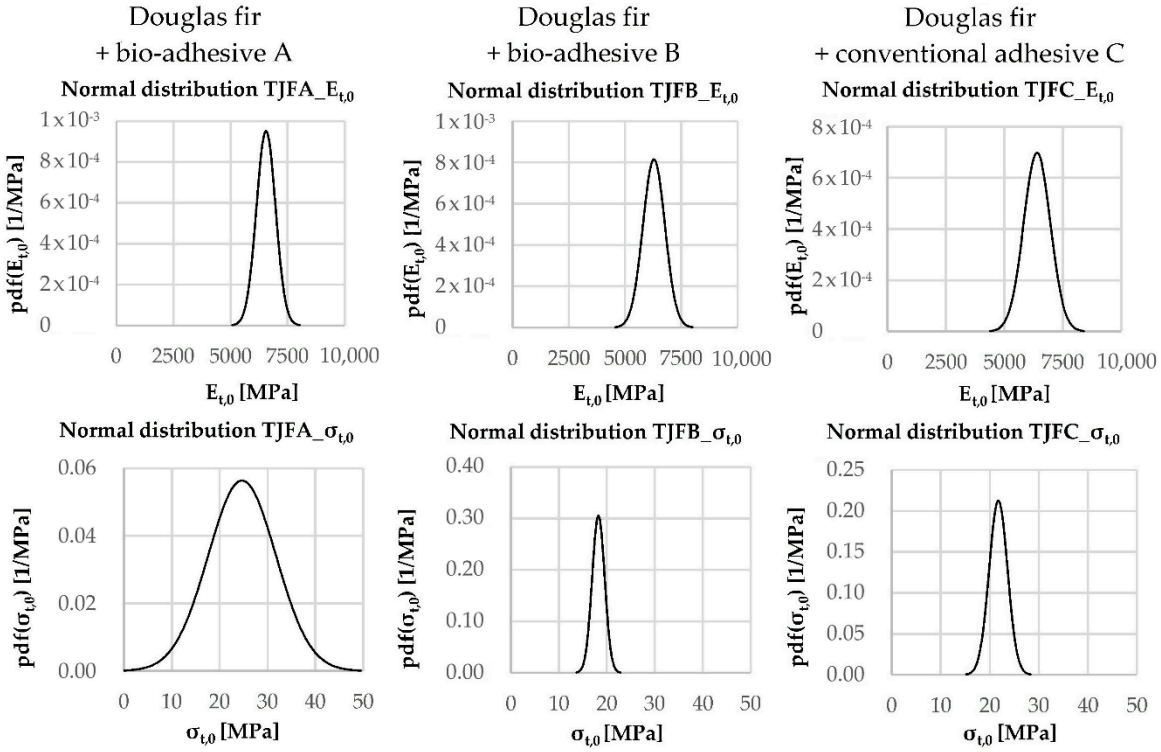

Figure A1. Statistical analysis for tensile properties on Douglas fir scarf-joint specimens.

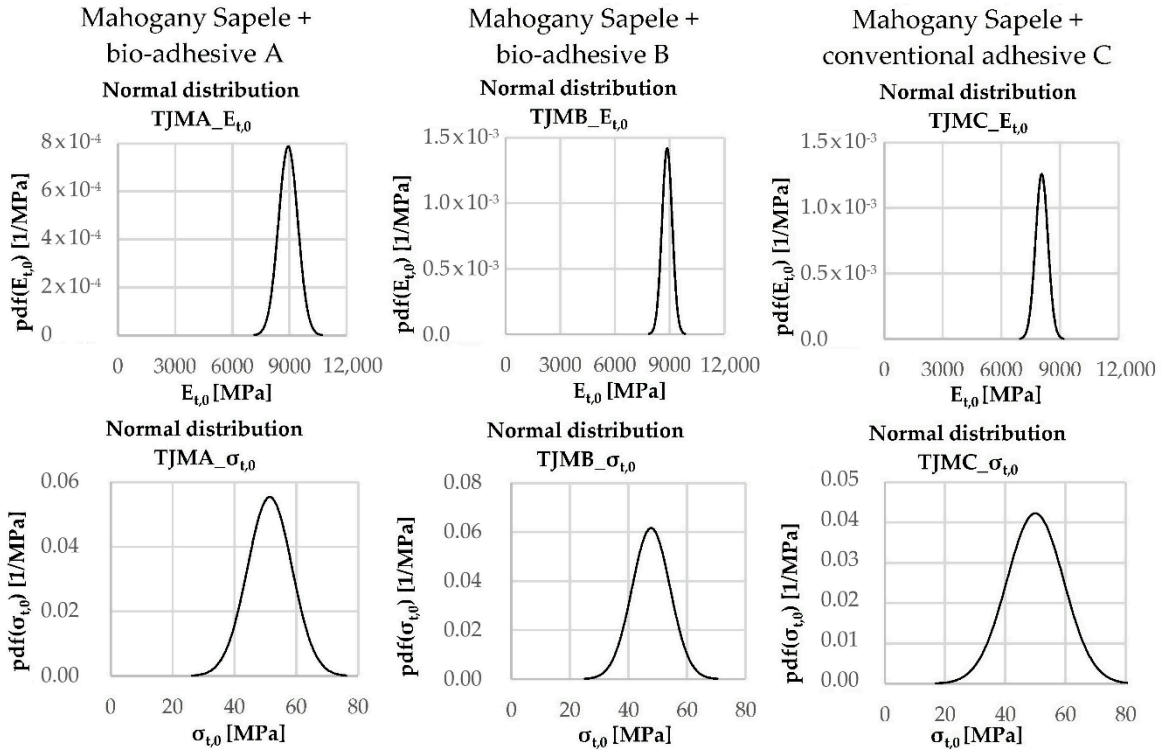

Figure A2. Statistical analysis for tensile properties on Mahogany Sapele scarf-joint specimens.

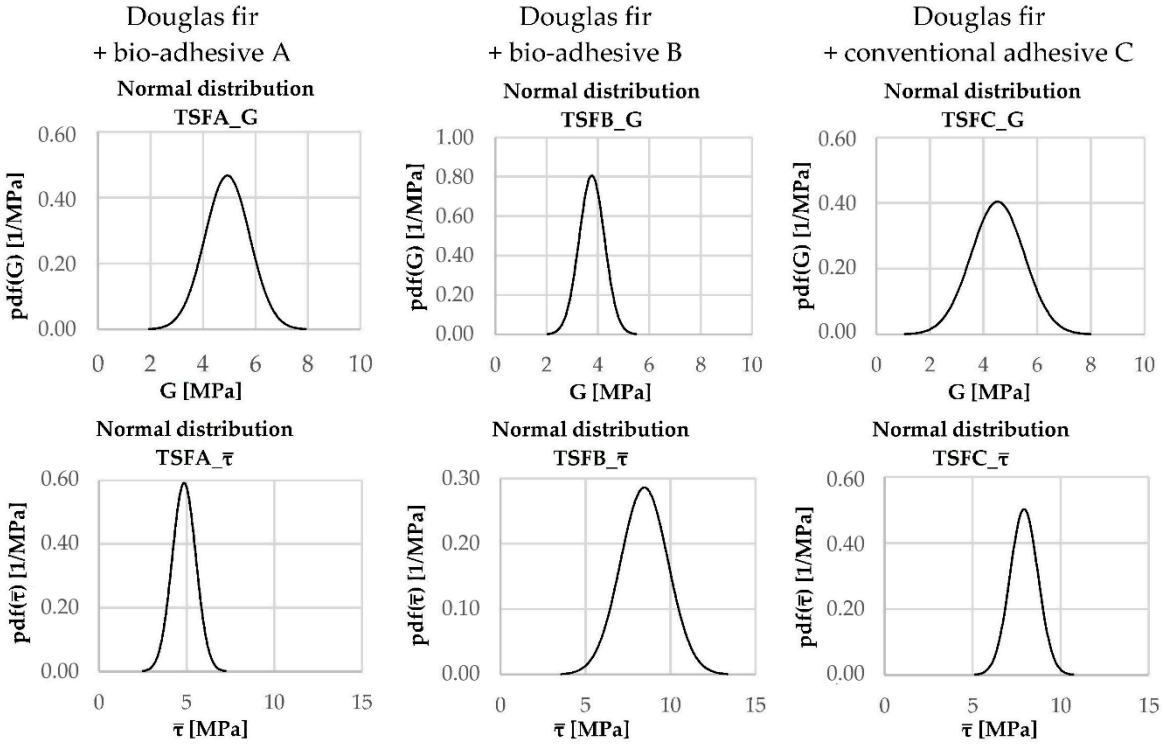

Figure A3. Statistical analysis for shear properties by tensile loading on Douglas fir lap joint specimens.

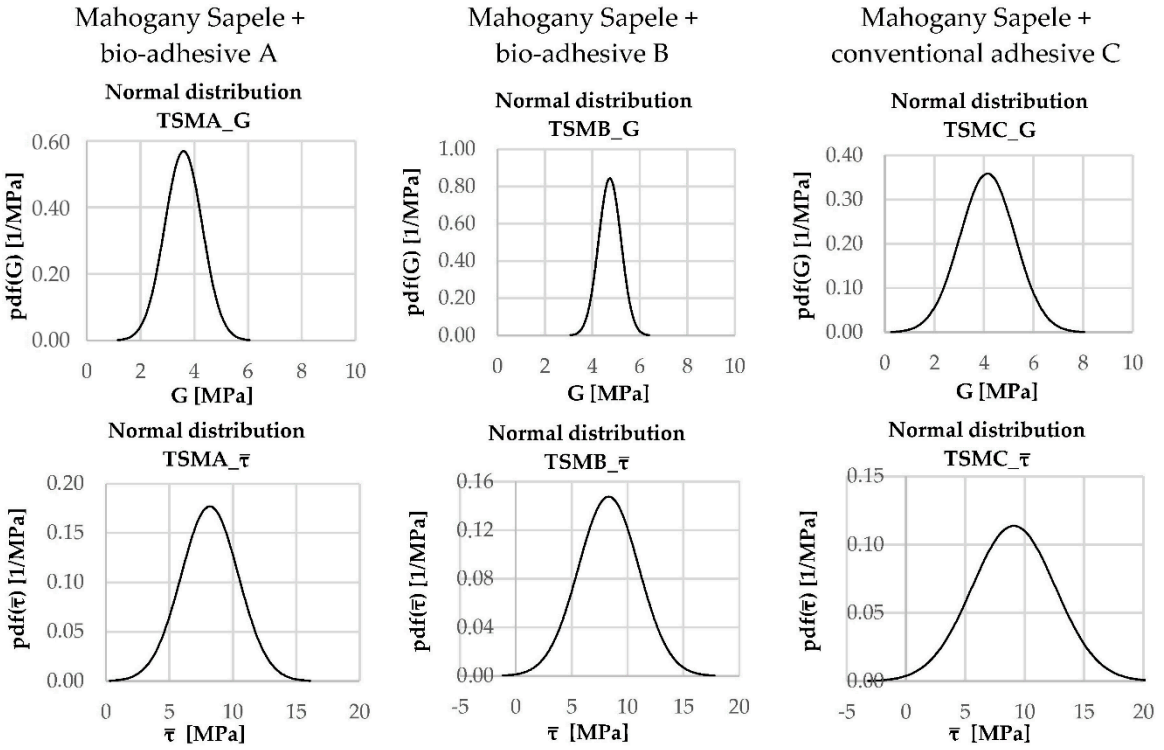

Figure A4. Statistical analysis for shear properties by tensile loading on Mahogany Sapele lap joint specimens.

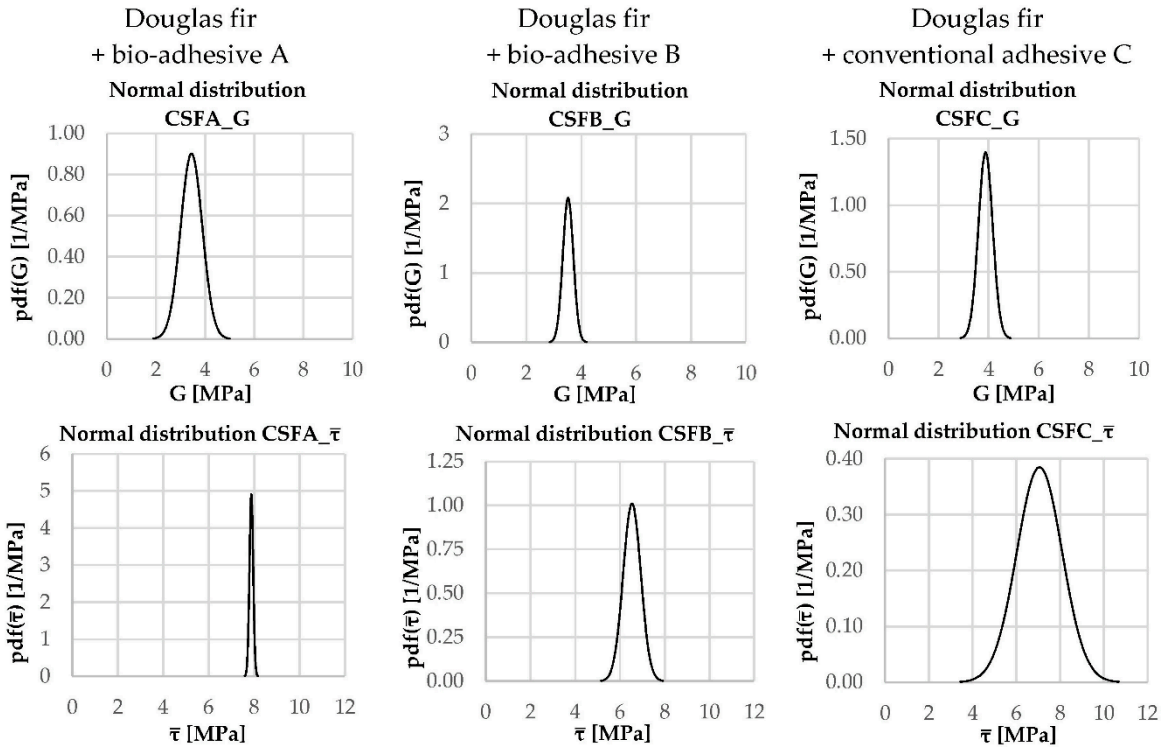

Figure A5. Statistical analysis for shear properties by compression loading on Douglas fir specimens.

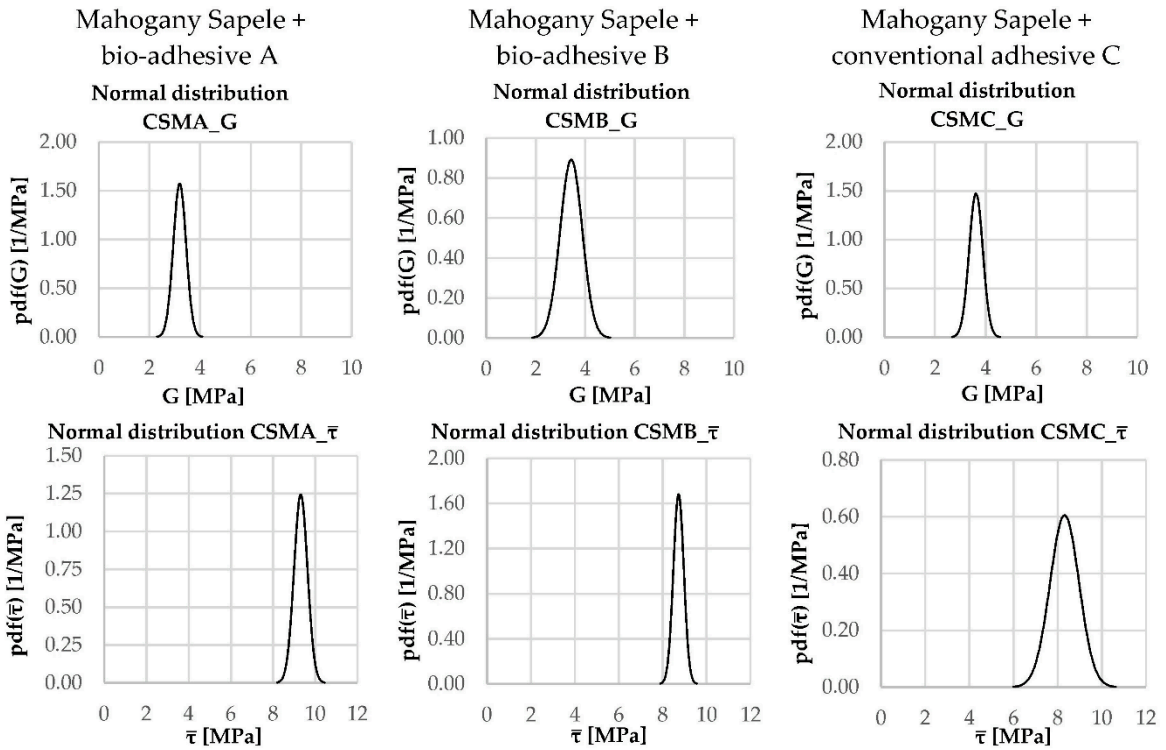

Figure A6. Statistical analysis for shear properties by compression loading on Mahogany Sapele specimens.

References

1. Rubino, F.; Nisticò, A.; Tucci, F.; Carlone, P. Marine application of fiber reinforced composites: A review. *J. Mar. Sci. Eng.* **2020**, *8*, 26. [CrossRef]
2. Weitzenböck, J. *Adhesives in Marine Engineering*, 1st ed.; Woodhead Publishing: Cambridge, UK, 2012.

3. Corigliano, P.; Ragni, M.; Castagnetti, D.; Crupi, V.; Dragoni, E.; Guglielmino, E.; Ragni, M.; Castagnetti, D.; Crupi, V.; Dragoni, E.; et al. Measuring the static shear strength of anaerobic adhesives in finite thickness under high pressure. *J. Adhes.* **2019**, 1–18. [CrossRef]
4. Grabovac, I. Bonded composite solution to ship reinforcement. *Compos. Part A Appl. Sci. Manuf.* **2003**, *34*, 847–854. [CrossRef]
5. Sapronov, O.; Maruschak, P.; Sotsenko, V.; Buketova, N.; Da Gloria De Deus, A.B.; Sapronova, A.; Prentkovskis, O. Development and use of new polymer adhesives for the restoration of marine equipment units. *J. Mar. Sci. Eng.* **2020**, *8*, 527. [CrossRef]
6. Kolat, K.; Neşer, G.; Özes, Ç. The effect of sea water exposure on the interfacial fracture of some sandwich systems in marine use. *Compos. Struct.* **2007**, *78*, 11–17. [CrossRef]
7. Nasso, C.; la Monaca, U.; Marinò, A.; Bertagna, S.; Bucci, V. The strip planking: An eco-friendly solution for the end-of-life of ships. In Proceedings of the NAV International Conference on Ship and Shipping Research, Trieste, Italy, 20–22 June 2018; IOS Press: Amsterdam, The Netherlands, 2018.
8. López, F.A.; Martín, M.I.; Alguacil, F.J.; Rincón, J.M.; Centeno, T.A.; Romero, M. Thermolysis of fibreglass polyester composite and reutilisation of the glass fibre residue to obtain a glass-ceramic material. *J. Anal. Appl. Pyrolys.* **2012**, *93*, 104–112. [CrossRef]
9. Nahil, M.A.; Williams, P.T. Recycling of carbon fibre reinforced polymeric waste for the production of activated carbon fibres. *J. Anal. Appl. Pyrolys.* **2011**, *91*, 67–75. [CrossRef]
10. Palmer, J.; Savage, L.; Ghita, O.R.; Evans, K.E. Sheet moulding compound (SMC) from carbon fibre recyclate. *Compos. Part A Appl. Sci. Manuf.* **2010**, *41*, 1232–1237. [CrossRef]
11. Pannkoke, K.; Oethe, M.; Busse, J. Efficient prepreg-recycling at low temperatures. *Asian Text. J.* **2000**, *9*, 70–74. [CrossRef]
12. Pickering, S.J. Recycling technologies for thermoset composite materials-current status. *Compos. Part A Appl. Sci. Manuf.* **2006**, *37*, 1206–1215. [CrossRef]
13. Vo Dong, P.A.; Azzaro-Pantel, C.; Cadene, A.L. Economic and environmental assessment of recovery and disposal pathways for CFRP waste management. *Resour. Conserv. Recycl.* **2018**, *133*, 63–75. [CrossRef]
14. Bose, S.; Vijith, V. Wooden Boat Building For Sustainable Development. *Int. J. Innov. Res. Dev.* **2012**, *1*, 345–360.
15. Önal, M.; Neşer, G. End-of-life alternatives of glass reinforced polyester boat hulls compared by LCA. *Adv. Compos. Lett.* **2018**, *27*, 134–141. [CrossRef]
16. Nasso, C.; La Monaca, U.; Bertagna, S.; Braidotti, L.; Mauro, F.; Trincas, G.; Marinó, A.; Bucci, V. Integrated design of an eco-friendly wooden passenger craft for inland navigation. *Int. Shipbuild. Prog.* **2019**, *66*, 35–55. [CrossRef]
17. Castegnaro, S.; Gomiero, C.; Battisti, C.; Poli, M.; Basile, M.; Barucco, P.; Pizzarello, U.; Quaresimin, M.; Lazzaretto, A. A bio-composite racing sailboat: Materials selection, design, manufacturing and sailing. *Ocean Eng.* **2017**, *133*, 142–150. [CrossRef]
18. Praharsi, Y.; Jami'in, M.A.; Suhardjito, G.; Wee, H.M. Modeling a traditional fishing boat building in East Java, Indonesia. *Ocean Eng.* **2019**, *189*, 106234. [CrossRef]
19. Lopez-Anido, R.; Michael, A.P.; Sandford, T.C. Experimental characterization of FRP composite-wood pile structural response by bending tests. *Mar. Struct.* **2003**, *16*, 257–274. [CrossRef]
20. Bucci, V.; Corigliano, P.; Crupi, V.; Epasto, G.; Guglielmino, E.; Marinò, A. Experimental investigation on Iroko wood used in shipbuilding. *Proc. Inst. Mech. Eng. Part C J. Mech. Eng. Sci.* **2017**, *231*. [CrossRef]
21. Corigliano, P.; Crupi, V.; Epasto, G.; Guglielmino, E.; Maugeri, N.; Marinò, A. Experimental and theoretical analyses of Iroko wood laminates. *Compos. Part B Eng.* **2017**, *112*. [CrossRef]
22. Yang, T.H.; Wang, S.Y.; Lin, C.J.; Tsai, M.J. Evaluation of the mechanical properties of Douglas-fir and Japanese cedar lumber and its structural glulam by nondestructive techniques. *Constr. Build. Mater.* **2008**, *22*, 487–493. [CrossRef]
23. Winandy, J.; Morrell, J. Relationship between incipient decay, strength, and chemical composition of Douglas-fir heartwood. *Wood Fiber Sci.* **1993**, *25*, 278–288.
24. Susainathan, J.; Eyma, F.; De Luycker, E.; Cantarel, A.; Castanie, B. Experimental investigation of impact behavior of wood-based sandwich structures. *Compos. Part A Appl. Sci. Manuf.* **2018**, *109*, 10–19. [CrossRef]
25. Demircioğlu, T.K.; Balıkoğlu, F.; İnal, O.; Arslan, N.; Ataş, A. Experimental investigation on low-velocity impact response of wood skinned sandwich composites with different core configurations. *Mater. Today Commun.* **2018**, *17*, 31–39. [CrossRef]
26. Nicolson, I. *Cold-Molded and Strip-Planked Wood Boatbuilding*; Adlard Coles Nautical: London, UK, 1991; ISBN 9780540071470.
27. Germanischer Lloyd, Rules for Classification and Construction. *Ship Technology*; DNV GL SE: Hamburg, Germany, 2011.
28. *UNI EN 350:2016-Durability of Wood and Wood-Based Products-Testing and Classification of the Durability to Biological Agents of Wood and Wood-Based Materials*; CEN: Brussels, Belgium, 2016.
29. DIN EN 408-Structural Timber and Glued Laminated Timber. *Determination of Some Physical and Mechanical Properties*; CEN: Brussels, Belgium, 2004.
30. *UNI EN 302-1-Adhesives for Load-Bearing Timber Structures-Test Methods-Part 1: Determination of Longitudinal Tensile Shear Strength*; SIST EN: Stockholm, Sweden, 2013.
31. *ASTM International D905-03: Standard Test Method for Strength Properties of Adhesive Bonds in Shear by Compression Loading*; ASTM International: West Conshohocken, PA, USA, 2003.